

Energy flows in thick accretion disks and their consequences for black hole feedback

Aleksander Sądowski^{1*}, Jean-Pierre Lasota^{2,3*}, Marek A. Abramowicz^{3,4*}
and Ramesh Narayan^{5*}

¹ MIT Kavli Institute for Astrophysics and Space Research 77 Massachusetts Ave, Cambridge, MA 02139, USA

² Institut d'Astrophysique de Paris, CNRS et Sorbonne Universités, UPMC Paris 06, UMR 7095, 98bis Bd Arago, 75014 Paris, France

³ Nicolaus Copernicus Astronomical Center, Bartycka 18, 00-716 Warsaw, Poland

⁴ Physics Department, Gothenburg University, SE-412-96 Göteborg, Sweden

⁵ Harvard-Smithsonian Center for Astrophysics, 60 Garden St., Cambridge, MA 02134, USA

20 June 2016

ABSTRACT

We study energy flows in geometrically thick accretion disks, both optically thick and thin, using general relativistic, three-dimensional simulations of black hole accretion flows. We find that for non-rotating black holes the efficiency of the total feedback from thick accretion discs is 3% - roughly half of the thin disc efficiency. This amount of energy is ultimately distributed between outflow and radiation, the latter scaling weakly with the accretion rate for super-critical accretion rates, and returned to the interstellar medium. Accretion on to rotating black holes is more efficient because of the additional extraction of rotational energy. However, the jet component is collimated and likely to interact only weakly with the environment, whereas the outflow and radiation components cover a wide solid angle.

Key words: accretion, accretion discs – black hole physics – relativistic processes – methods: numerical

1 INTRODUCTION

Several aspects of the evolution of galaxies have been puzzling astronomers for decades. Firstly, star formation in galaxies turns out to be efficiently quenched in galactic bulges despite the gas cooling time being much shorter than the age of a given galaxy (Cowie & Binney 1977; Fabian & Nulsen 1977). Secondly, the galaxy luminosity function features a sharp high-mass cutoff in which the most massive systems are red, dead and elliptical, inconsistent with the hierarchical growth of structure in the Universe (Croton et al. 2006). Explaining both phenomena requires additional processes preventing gas from collapsing into stars and limiting the mass of the central galaxies.

Supernova explosions and stellar winds return energy (provide *feedback*) to the interstellar medium (ISM). Although these processes take place at small scales, they are powerful enough to affect the evolution of the whole galaxy. Without strong stellar feedback, gas inside galaxies would cool efficiently and collapse on a dynamical time resulting in star formation rates inconsistent with observations. As shown recently shown by Hopkins et al. (2014), stellar feedback itself is enough to explain most of the properties of galax-

ies, e.g., the relation between galaxy stellar mass and halo mass, at stellar masses $M_* \lesssim 10^{11} M_\odot$.

Additional processes are needed to explain the formation of the most massive galaxies. It is believed that almost every galaxy harbours a supermassive black hole (SMBH) in its nucleus. Being extremely compact such objects can liberate gravitational energy in large amounts. As a black hole (BH) grows to 0.2% of the bulge mass through accreting matter, it releases nearly 100 times the gravitational binding energy of its host galaxy (Fabian et al. 2009). It is therefore reasonable to expect that, if only the energy returned from accretion (the *black hole feedback*) is efficiently coupled with the ISM, the central SMBHs can strongly affect the formation and the properties of the host galaxies.

The feedback provided by SMBHs is therefore crucial for studying the evolution of the Universe. It is often accounted for in large scale simulations of galaxy formation, but the adopted models are very simplistic. The large range of scales involved in such simulations does not allow for detailed numerical (and simultaneous) modeling of the BH accretion. Instead, the mass supply rate is estimated (at most) at parsec scales, usually using the Bondi model of spherical accretion, and simple formulae for the feedback efficiency are applied. These are based partly on the standard thin disc models (Shakura & Sunyaev 1973), but (to be consistent with observed properties of galaxies) involve additional factors arbitrarily rescaling the feedback rate.

These factors reflect our lack of understanding of how accre-

* E-mail: asadowsk@mit.edu (AS); lasota@iap.fr (JPL); marek.abramowicz@physics.gu.se (MAA); rnarayan@cfa.harvard.edu (RN)

tion on SMBHs works and the efficiency of the feedback it provides. There are two major unknown. Firstly, it is not clear how much matter makes it to the BH, and how much is lost on the way. In other words, what fraction of the gas attracted by the BH near the Bondi radius ultimately crosses the BH horizon and efficiently liberates its binding energy providing the energy source for the feedback (see discussion in Yuan & Narayan 2014). Secondly, it is crucial to understand what fraction of this energy is returned to the ISM.

In this paper we address the second question. The feedback efficiency from an accretion flow is believed to be well established only for geometrically thin discs, corresponding to moderate, sub-Eddington accretion rates, $10^{-3}\dot{M}_{\text{Edd}} \lesssim \dot{M} \lesssim \dot{M}_{\text{Edd}}$ (for the definition of \dot{M}_{Edd} see Eq. 26). In this case, the accretion flow is radiatively efficient, and all the released binding energy of the gas¹ goes into radiation and is determined by the binding energy of the gas at the disc's inner edge (e.g., it equals 5.7% of the accreted rest mass energy, $\dot{M}c^2$, for a non-rotating BH).

We address here the question of what amount of energy is extracted if accretion flows are not geometrically thin, i.e., how efficient the BH feedback is if a SMBH accretes either in the radio mode ($\dot{M} \lesssim 10^{-3}\dot{M}_{\text{Edd}}$), when one expects an optically thin accretion flow and low radiative efficiency, or above the Eddington accretion rate, in an optically thick disc. To this purpose, we analyze a set of state-of-the-art, three-dimensional simulations of the innermost region of BH accretion performed with a general-relativistic, radiative magnetohydrodynamical (MHD) code KORAL (Sądowski et al. 2013).

Our paper has the following structure. In Section 2 we discuss the energy transfer in the standard model of a thin disc. In Section 3 we give the details of the numerical simulations and discuss their properties. In Section 4 we discuss their implications and several caveats. Finally, in Section 5 we summarize our findings.

2 ENERGY FLOW IN THIN DISCS

We start by recapitulating the physics of energy transfer in the standard model of a thin accretion disc (e.g. Shakura & Sunyaev 1973; Frank et al. 1992). This will give us a good reference point when discussing energy flows in numerical simulations of accretion flows.

2.1 Viscous dissipation

The thin disc model assumes Keplerian azimuthal motion, small vertical thickness of the disc, $h/r \ll 1$, and radiative efficiency. Keplerian angular velocities imply differential rotation and, in the presence of viscosity, non-zero transfer of angular momentum between adjacent rings. The torque exerted by rings on each other is (Frank et al. 1992),

$$T = 2\pi r \nu \Sigma r^2 \frac{d\Omega}{dr} = -3\pi \nu \Sigma r^2 \Omega, \quad (1)$$

where Σ is the surface density at radius r , $\Omega = \sqrt{GM/r^3}$ is the Keplerian angular velocity, and ν is the local kinematic viscosity coefficient corresponding to magnetically induced turbulence.

¹ The accretion itself is not the only energy source in an accreting system. If the accretion manages to bring a significant amount of magnetic flux on the BH, magnetic jets can extract rotational energy of the BH. Jets, however, are collimated, and may not interact efficiently with the ISM.

The torque results in transfer of angular momentum between the rings. Conservation of angular momentum requires,

$$\frac{d}{dr} \dot{M} \Omega r^2 = -\frac{dT}{dr}, \quad (2)$$

where $\dot{M} > 0$ denotes the accretion rate. Integrating between radius r and the inner edge of the disc at r_{in} , we get,

$$-\dot{M} (\Omega(r)r^2 - \Omega(r_{\text{in}})r_{\text{in}}^2) = T(r) - T(r_{\text{in}}). \quad (3)$$

Following the standard assumption that the torque at the inner edge of a thin disc vanishes (see Paczyński 2000) we get,

$$T = -\sqrt{GM\dot{M}} (\sqrt{r} - \sqrt{r_{\text{in}}}). \quad (4)$$

This torque not only transports angular momentum but also dissipates mechanical energy heating up the gas. The dissipation rate (per unit radius) in the whole ring which equals, by assumption of radiative efficiency, minus the radiative cooling rate, is given by,

$$q_{\text{diss}} = -q_{\text{rad}} = -T \frac{d\Omega}{dr} = -\frac{3GM\dot{M}}{2r^2} \left(1 - \sqrt{\frac{r_{\text{in}}}{r}}\right), \quad (5)$$

where the signs have been chosen such that a positive rate corresponds to cooling, and negative to heating. Dividing by the surface area of both sides of the ring we get the well known thin-disc surface radiative flux,

$$Q_{\text{rad}} = \frac{q_{\text{rad}}}{4\pi r} = \frac{3GM\dot{M}}{8\pi r^3} \left(1 - \sqrt{\frac{r_{\text{in}}}{r}}\right). \quad (6)$$

It is worth reiterating that the viscous dissipation rate (the gas heating rate) does not depend on the particular form of the viscosity (e.g., the α -viscosity), but follows from the assumptions of Keplerian motion, the zero-torque boundary condition and angular momentum conservation.

2.2 Local energy budget

In the previous paragraph we have shown that viscous dissipation in a differentially rotating flow results in heating of gas and radiative cooling at the rate q_{rad} (Eq. 5).

The energy required for this radiative emission may come from the gravitational field – gas approaching the BH liberates its own binding energy at the rate,

$$q_{\text{bind}} = \dot{M} \frac{de_{\text{bind}}}{dr} = \dot{M} \frac{d}{dr} \left(-\frac{GM}{2r}\right) = \frac{GM\dot{M}}{2r^2}. \quad (7)$$

However, it is clear that,

$$q_{\text{bind}} + q_{\text{rad}} \neq 0. \quad (8)$$

This means that there must be another source or sink component in the local budget of energy.

In the previous section we have seen that viscosity leads to the transport of angular momentum and dissipation of mechanical energy. However, viscosity transports not only angular momentum but also rotational energy. The amount of energy transported in this way is,

$$L_{\text{visc}} = -T\Omega, \quad (9)$$

and the resulting local heating or cooling rate per unit radius is given by,

$$q_{\text{visc}} = \frac{d}{dr}(T\Omega) = \frac{GM\dot{M}}{r^2} \left(1 - \frac{3}{2} \sqrt{\frac{r_{\text{in}}}{r}}\right). \quad (10)$$

It is straightforward to verify that,

$$q_{\text{bind}} + q_{\text{rad}} + q_{\text{visc}} = 0. \quad (11)$$

The viscous energy transport redistributes energy released in the disc and compensates for the imbalance between the local binding energy release and the rate of radiative cooling.

In Fig. 1 we plot local heating/cooling rates in a thin disc as a function of radius. The solid blue line shows the energy gain from the change in the binding energy, q_{bind} (Eq. 7). This quantity is further decomposed into the gravitational,

$$q_{\text{grav}} = \dot{M} \frac{de_{\text{grav}}}{dr} = \dot{M} \frac{d}{dr} \left(-\frac{GM}{r} \right) = \frac{GM\dot{M}}{r^2}, \quad (12)$$

and kinetic,

$$q_{\text{kin}} = \dot{M} \frac{de_{\text{kin}}}{dr} = \dot{M} \frac{d}{dr} \left(\frac{GM}{2r} \right) = -\frac{GM\dot{M}}{2r^2}. \quad (13)$$

components. They are denoted by dashed and dotted blue lines, respectively.

The orange line shows the radiative cooling rate, q_{rad} (Eq. 5). As expected, no emission comes from the inner edge of the disc (located at $r_{\text{in}} = 6GM/c^2$, but we are using here the Newtonian approximation) and the most efficient emission takes place from a ring located at $r \approx 8r_g^2$, where $r_g = GM/c^2$.

The pink line reflects the energy redistribution rate by the viscosity, q_{visc} (Eq. 10). For $r \lesssim 13r_g$ it is negative – at these radii viscosity effectively cools the disc and carries the energy outward. It is particularly evident for the gas approaching the inner edge, where the release of binding energy is large, but the no-torque boundary condition prevents radiative emission. To maintain the energy balance, viscosity must transport this locally liberated binding energy out.

For $r \gtrsim 13r_g$, q_{visc} becomes positive, which means that the viscous energy flux decreases with increasing radius and locally deposits energy, contributing to the local heating rate and increasing the magnitude of radiative cooling beyond the rate at which local binding energy is liberated. In the limit $r \gg r_{\text{in}}$ one has $q_{\text{rad}} = -3q_{\text{bind}}$, i.e., the local rate of releasing energy in radiation is three times larger than the change in binding energy. The extra contribution comes from the viscous energy flux which deposit energy (and heats up gas) at a rate two times larger than the gain from released binding energy.

2.3 Energy flow

In the previous section we have looked into the local energy balance. Now, let us look into the total amount of energy carried by its various components from one radius to another.

The binding energy is carried by the flow at a rate,

$$L_{\text{bind}} = -\dot{M}e_{\text{bind}} = \frac{GM\dot{M}}{2r} > 0, \quad (14)$$

where the positive sign reflects the fact that bound gas is falling inward, thus effectively depositing energy at infinity. The luminosity in binding energy may be again decomposed into the gravitational and kinetic components,

$$L_{\text{grav}} = -\dot{M}e_{\text{grav}} = \frac{GM\dot{M}}{r} > 0, \quad (15)$$

² The maximum is at $r = (49/6)r_g$.

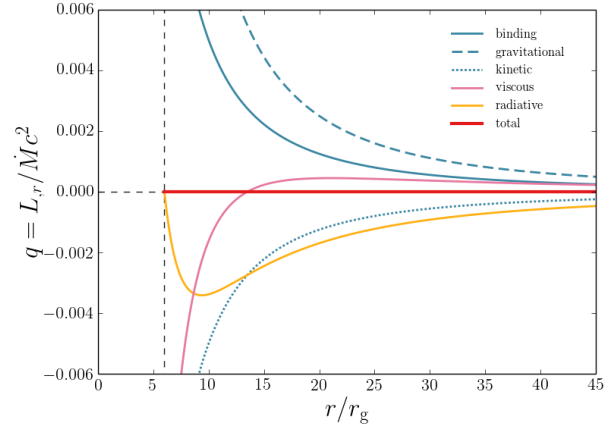


Figure 1. Local energy gain in its various forms in the standard thin disc model described in Section 2.

$$L_{\text{kin}} = -\dot{M}e_{\text{kin}} = -\frac{GM\dot{M}}{2r} < 0. \quad (16)$$

Gravitational energy luminosity is positive, but the kinetic luminosity is negative – kinetic energy of the Keplerian motion is brought inward by the gas.

The radiative cooling rate, q_{rad} , is given by Eq. 5. Photons are emitted from the disc surface and leave the system. The total radiative luminosity at given radius, L_{rad} , results from the emission inside that radius,

$$L_{\text{rad}} = \int_{r_{\text{in}}}^r q_{\text{rad}} dr = \frac{3}{2} \frac{GM\dot{M}}{r} \left(\frac{1}{3} \frac{r}{r_{\text{in}}} + \frac{2}{3} \sqrt{\frac{r_{\text{in}}}{r}} - 1 \right) > 0. \quad (17)$$

This quantity is zero at the inner edge ($r = r_{\text{in}}$) and equals $GM\dot{M}/2r_{\text{in}}$ at infinity. The radiative luminosity of the whole accretion disc is therefore equal to the binding energy of the gas crossing the inner edge.

Finally, the amount of energy carried by viscosity from the inner region outward, L_{visc} , is (Eq. 9),

$$L_{\text{visc}} = -T\Omega = \frac{GM\dot{M}}{r} \left(1 - \sqrt{\frac{r_{\text{in}}}{r}} \right) > 0. \quad (18)$$

The various integrated energy fluxes introduced above are shown in Fig. 2. Their magnitudes have been normalized to the amount of accreted rest-mass energy. The blue lines show the luminosities in the binding energy, L_{bind} , and its gravitational and kinetic components, L_{grav} and L_{kin} . At the inner edge ($r_{\text{in}} = 6r_g$), the amount of binding energy carried by the gas is

$$L_{\text{bind,in}} = \frac{GM\dot{M}}{2r_{\text{in}}} = \frac{1}{12} \dot{M}c^2, \quad (19)$$

which is, as we will discuss in detail in a moment, the total efficiency of a thin disc in the Newtonian gravitational potential.

The orange line in Fig. 2 shows the radiative luminosity crossing a sphere of radius r . As no photons are emitted from inside the inner edge, it starts from zero and gradually grows, reaching finally $GM\dot{M}/2r_{\text{in}}$ at infinity – in a thin disc, the whole energy extracted by the infalling gas ultimately goes into radiation.

It is interesting to note that 50% of the radiation is emitted from outside $r \approx 25r_g$. At the same time, the gas infalling from infinity down to that radius has extracted only roughly 25% of the available binding energy. The excess in radiative luminosity comes from the extra energy carried by viscosity from the innermost region.

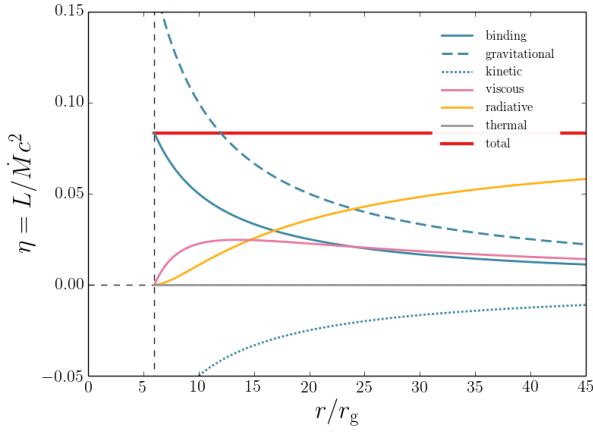


Figure 2. Luminosity in various forms of energy for the standard thin disc model described in Section 2. The thick red line denotes the total luminosity of the system which can be decomposed into the luminosity in binding energy (solid blue line), in radiation (orange) and luminosity transported by viscosity (pink). The luminosity in binding energy is further decomposed into gravitational (blue dashed) and kinetic (blue dotted) components. All the luminosities are normalized with the accreted rest-mass energy, $\dot{M}c^2$.

This component of the energy flux is denoted with the pink line at the same plot. The amount of energy carried by viscosity grows rapidly just outside of the inner edge – at these radii viscosity is transporting rotational kinetic energy outward. Outside $r \approx 13r_g$ the luminosity of viscous energy transport drops down with radius and the energy taken away from the innermost region is deposited by viscosity into the gas.

Summing up all the components of the energy transfer we get the total luminosity,

$$L_{\text{tot}} = L_{\text{bind}} + L_{\text{rad}} + L_{\text{visc}}, \quad (20)$$

which is the quantity that is fundamentally conserved in stationary flows, i.e., is independent of radius and no energy accumulates at any location. Indeed, the sum of the three components (red line in Fig. 2) gives a constant value equal to the total efficiency of accretion and the binding energy carried in by the gas through the disc inner edge $(1/12)\dot{M}c^2$. In the Schwarzschild metric this efficiency would be $\sim 0.057\dot{M}c^2$.

3 ENERGY FLOW IN SIMULATIONS OF ACCRETION FLOWS

Having recapitulated how energy flows in a standard thin disc, we are ready to study the energy redistribution in numerical simulations of accretion flows. In the following Section we describe the numerical method used to perform the simulations. In Section 3.2 we introduce the formalism used to study energy fluxes in numerical solutions. In Sections 3.3 and 3.4 we look in detail into the energy flow in simulations of optically thin and thick discs, respectively.

3.1 Numerical setup

The simulations analyzed in this paper were performed in three dimensions with the general relativistic radiation magnetohydrodynamical (GRRMHD) code KORAL (Sądowski et al. 2013) which

solves the conservation equations in a fixed, arbitrary spacetime using finite-difference methods. The equations we solve are,

$$(\rho u^\mu)_{;\mu} = 0, \quad (21)$$

$$(T^\mu_\nu)_{;\mu} = G_\nu, \quad (22)$$

$$(R^\mu_\nu)_{;\mu} = -G_\nu, \quad (23)$$

where ρ is the gas density in the comoving fluid frame, u^μ are the components of the gas four-velocity, T^μ_ν is the MHD stress-energy tensor,

$$T^\mu_\nu = (\rho + u_g + p_g + b^2)u^\mu u_\nu + (p_g + \frac{1}{2}b^2)\delta^\mu_\nu - b^\mu b_\nu, \quad (24)$$

R^μ_ν is the stress-energy tensor of radiation, and G_ν is the radiative four-force describing the interaction between gas and radiation (see Sądowski et al. 2014, for a more detailed description). Here, u_g and $p_g = (\Gamma - 1)u_g$ represent the internal energy and pressure of the gas in the comoving frame and b^μ is the magnetic field 4-vector (Gammie et al. 2003). The magnetic pressure is $p_{\text{mag}} = b^2/2$ in geometrical units.

The magnetic field is evolved via the induction equation,

$$\partial_t(\sqrt{-g}B^i) = -\partial_j(\sqrt{-g}(b^j u^i - b^i u^j)), \quad (25)$$

where B^i is the magnetic field three-vector (Komissarov 1999), and $\sqrt{-g}$ is the metric determinant. The divergence-free criterion is enforced using the flux-constrained scheme of Tóth (2000).

The radiation field is evolved through its energy density and flux, and the radiation stress-energy tensor is closed by means of the M1 closure scheme (Levermore 1984; Sądowski et al. 2013). The energy exchange between gas and radiation is by free-free emission/absorption as well as Compton scattering. The latter is treated in the “blackbody” Comptonization approximation as described in Sądowski et al. (2015c).

We use modified Kerr-Shild coordinates with the inner edge of the domain inside the BH horizon. The simulations are run with a moderately high resolution of 252 grid cells spaced logarithmically in radius, 234 grid cells in the polar angle, concentrated towards the equatorial plane, and 128 cells in azimuth.

Three of the four simulations which we analyze in this work are identical to the ones presented in Sądowski et al. (2015d). To have a consistent optically thin version of an accretion flow we simulated an additional model with purely magnetohydrodynamical evolution, i.e., without radiation field. This simulation (h001) corresponds to an optically thin, advection dominated accretion flows (ADAF) believed to occur in systems accreting well below the Eddington level (Yuan & Narayan 2014).

Parameters of the models are given in Table 1.

In this work we adopt the following definition for the Eddington mass accretion rate,

$$\dot{M}_{\text{Edd}} = \frac{L_{\text{Edd}}}{\eta c^2}, \quad (26)$$

where $L_{\text{Edd}} = 1.25 \times 10^{38} M/M_\odot$ ergs/s is the Eddington luminosity, and η is the radiative efficiency of a thin disc around a black hole with a given spin $a_* \equiv a/M$. For zero BH spin, $\dot{M}_{\text{Edd}} = 2.48 \times 10^{18} M/M_\odot$ g/s. Hereafter, we also use the gravitational radius $r_g = GM/c^2$ as the unit of length, and r_g/c as the unit of time.

In this study we consider simulation output averaged over time. Therefore, whenever we write, e.g., ρu^r , we mean the average of the product, i.e., $\langle \rho u^r \rangle$, where $\langle \rangle$ stands for time averaging.

Table 1. Model parameters

	h001	r001	r003	r011
	hydro	radiative	radiative	radiative
M_{BH}	$10M_{\odot}$	$10M_{\odot}$	$10M_{\odot}$	$10M_{\odot}$
$\dot{M}/\dot{M}_{\text{Edd}}$	$\lesssim 10^{-3}$	10.0	175.8	17.4
a_*	0.0	0.0	0.0	0.7
t_{max}	23,000	20,000	19,000	16,100

All models initiated as in Sądowski et al. (2015d).

M_{BH} - mass of the BH, \dot{M} - average accretion rate,

a_* - nondimensional spin parameter,

t_{max} - duration of the simulation in units of GM/c^3

3.2 Energy fluxes

3.2.1 Fundamental quantities

In quasi-stationary state the accretion rate is constant in radius, i.e., gas does not accumulate anywhere, but rather flows towards the BH with constant rate. The accretion rate (the luminosity in rest-mass energy) is given by,

$$\dot{M} = \int_0^{\pi} \int_0^{2\pi} \sqrt{-g} \rho u^r d\phi d\theta, \quad (27)$$

where this and the following integrals are evaluated at a fixed radius r .

In a similar way we may define the luminosity in all forms of energy,

$$L_{\text{tot},0} = - \int_0^{\pi} \int_0^{2\pi} \sqrt{-g} (T_t^r + R_t^r) d\phi d\theta, \quad (28)$$

where we integrate the radial flux of energy carried by gas (T_t^r) and by radiation (R_t^r). This quantity, however, is not interesting from the point of view of a distant observer. It contains the flux of rest-mass energy which, even if deposited at infinity, will not have observational consequences (since at infinity rest-mass cannot be converted into other forms of energy in a trivial way). Therefore, we define the *total luminosity* by subtracting³ the rest-mass energy flux from the previous definition,

$$L_{\text{tot}} = - \int_0^{\pi} \int_0^{2\pi} \sqrt{-g} (T_t^r + R_t^r + \rho u^r) d\phi d\theta, \quad (29)$$

The sign has been chosen in such a way that L_{tot} is negative for energy falling in the BH, and positive for energy leaving the system.

In a stationary state the total luminosity is independent of radius (if it was not, energy would accumulate in some regions). It is the luminosity of the whole system, i.e., it is also the luminosity as seen from infinity. Therefore, it determines the rate at which energy is deposited in the interstellar medium or, in other words, L_{tot} is the total power of *feedback*.

3.2.2 Decomposition

The total energy flux consists of multiple components. We decompose it in a way which gives well-known Newtonian limits.

First, we single out the radiative component and define the radiative luminosity,

$$L_{\text{rad}} = - \int_0^{\pi} \int_0^{2\pi} \sqrt{-g} R_t^r d\phi d\theta, \quad (30)$$

³ Lower time index introduces a negative sign in T_t^r , so to get rid of the rest-mass component in T_t^r one has to *add* ρu^r .

which reflects energy carried by photons, either trapped in the gas, or propagating freely. To define other components, let us first write explicitly,

$$T_t^r + \rho u^r = \rho u^r (1 + u_t) + (\Gamma u_g + b^2) u^r u_t - b^r b_t. \quad (31)$$

Here we remind the reader that in all the integrals we take averages of products, e.g., $\rho u^r (1 + u_t)$ is actually $\langle \rho u^r (1 + u_t) \rangle$, where the product is averaged over time. This particular quantity is the average radial flux of binding energy. In detail, it is the sum of advective, $\langle \rho u^r \rangle \langle 1 + u_t \rangle$, and Reynolds (turbulent), $\langle \rho u^r (1 + u_t) \rangle - \langle \rho u^r \rangle \langle 1 + u_t \rangle$, components. Similar decomposition applies to the other components of the total energy flux. In this work we will not discriminate between the turbulent and advective fluxes, but instead focus on the net contribution.

It is straightforward to define the luminosity in internal (thermal) energy,

$$L_{\text{int}} = - \int_0^{\pi} \int_0^{2\pi} \sqrt{-g} \Gamma u_g u^r u_t d\phi d\theta, \quad (32)$$

which, similarly, contains the advective and convective terms, and the luminosity carried by the magnetic field,

$$L_{\text{magn}} = - \int_0^{\pi} \int_0^{2\pi} \sqrt{-g} (b^2 u^r u_t - b^r b_t) d\phi d\theta. \quad (33)$$

which again includes both the advective component and turbulent stress. The remaining term (proportional to $(1 + u_t)$) contains information about the gravitational and kinetic energies. In the Newtonian limit it gives $-1/2r$ for Keplerian motion. Therefore, we identify the corresponding integrated energy flux as the luminosity in binding energy carried radially by gas,

$$L_{\text{bind}} = - \int_0^{\pi} \int_0^{2\pi} \sqrt{-g} \rho u^r (1 + u_t) d\phi d\theta. \quad (34)$$

The gravitational component of the last expression can be singled out by calculating the specific binding energy $(1 + u_t)$ for a stationary observer. From $u^\mu = (u^t, \vec{0})$ and $u^\mu u_\mu = -1$ one gets (for a diagonal metric) $u_t = -\sqrt{-g_{tt}}$, and therefore, the luminosity in gravitational energy carried by gas is,

$$L_{\text{grav}} = - \int_0^{\pi} \int_0^{2\pi} \sqrt{-g} \rho u^r (1 - \sqrt{-g_{tt}}) d\phi d\theta. \quad (35)$$

The remaining term reflects the luminosity in kinetic energy,

$$L_{\text{kin}} = L_{\text{bind}} - L_{\text{grav}}. \quad (36)$$

To sum up, we have decomposed the total energy transfer rate into binding, thermal, magnetic, and radiative components,

$$L_{\text{tot}} = L_{\text{bind}} + L_{\text{int}} + L_{\text{magn}} + L_{\text{rad}}. \quad (37)$$

3.2.3 Advective and viscous energy fluxes

In a viscous accretion flow energy is transported both by viscosity and by the fluid which advectively carries energy with itself. One may write, $L_{\text{hydro}} = L_{\text{adv}} + L_{\text{visc}} = \dot{M} B e - T \Omega$, where $B e$ is the Bernoulli function of the fluid (which is not constant, because work is done on gas on its way towards the BH), and $T \Omega$ reflects the viscous rate of energy flow (Eq. 18). The hydrodynamical quantities defined in the previous section (L_{bind} , L_{int} , L_{magn}) are based on time averaged quantities. The turbulence, which provides effective viscosity, is averaged out and contributes to the energy transfer rate. Therefore, as stated in the previous Section, these luminosities include both terms, the advective and the viscous one. It is beyond the

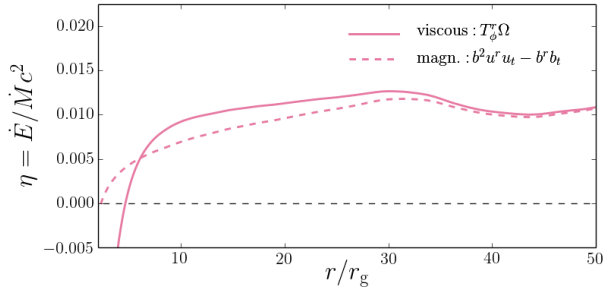


Figure 3. Total estimated viscous flux of energy (solid line), and the energy carried by magnetic fields, L_{magn} (Eq. 33, dashed line).

scope of this paper to decompose them and single out the energy transfer rate solely due to viscosity.

We estimated the viscous component by calculating⁴.

$$L_{\text{visc,est}} = - \int_0^\pi \int_0^{2\pi} \sqrt{-g} (T_\phi^r \Omega) d\phi d\theta. \quad (38)$$

This quantity is plotted in Fig. 3 with the pink solid line. In the same figure, we plot the magnetic component of the luminosity, L_{magn} (Eq. 33). The two have very similar profiles and magnitudes. This should not be surprising, because it is mostly magnetic field which mediates angular momentum transfer (local shearing sheet and global simulations of magnetized accretion show that the magnetic stress dominates over the Reynolds stress by a factor of ~ 4 , see Pessah et al. 2006; Penna et al. 2013b). From now on, we will consider the luminosity in the magnetic component, L_{magn} , as the counterpart of the viscous luminosity L_{visc} introduced in Section 2. Such assignment is helpful, but not crucial, for the following considerations.

Often in the literature (e.g. Abramowicz et al. 1988; Narayan & Yi 1994) the energy balance is written in the comoving frame in the following form,

$$\hat{q}^{\text{heating}} - \hat{q}^{\text{cooling}} = \hat{q}^{\text{adv}}, \quad (39)$$

where \hat{q}^{heating} and \hat{q}^{cooling} stand for local comoving heating and cooling rates, and \hat{q}^{adv} describes the net amount of heat taken away with the fluid or effectively brought in and locally released. This particular decomposition is not very helpful for the present study. However, we note that for both the optically thin and thick discs, as will be discussed below, the power advected with the fluid (in thermal and radiative energies, respectively) dominates the energy balance. Therefore, the flows discussed below are indeed advection dominated.

3.3 Energy flow in optically thin ADAFs

Let us now look at the energy flow in simulated, multi-dimensional accretion flows. We start with an optically thin disc (ADAF), model **h001**.

According to the standard model (Narayan & Yi 1994; Abramowicz et al. 1995) for this mode of accretion, energy locally

⁴ If the viscous stress is proportional to shear then it is orthogonal to the gas velocity, $T_{\text{visc},\nu}^\mu u^\nu = 0$. For purely azimuthal motion, $u^\mu = (u^t, 0, 0, u^\phi)$, one finds that $T_\phi^r \Omega = -T_r^t$. Therefore, $T_\phi^r \Omega$ indeed gives the radial flux of energy carried by viscosity. However, in the simulations we performed, the orthogonality and perfectly circular motion are not enforced and these conditions are only approximately satisfied.

dissipated does not have a chance to escape because of low radiative efficiency and is advected with the flow. This fact makes such discs very hot and geometrically thick. As a result, the expected efficiency of accretion is zero because all the binding energy gained by gas on its way towards the BH is balanced by thermal energy advected with it on the BH.

This model, however, does not allow the gas to flow out of the system. This process, in principle, can provide a path for the liberated binding energy to escape from the system, and as a result may increase the efficiency of accretion.

3.3.1 Luminosities

Figure 4 presents the integrated radial fluxes (luminosities) of energy in various forms for the optically thin simulation **h001**. The amount of binding energy (Eq. 34) carried with the flow is shown with solid blue line. The closer the gas gets to the BH, the more bound it is, and the more luminosity it extracts with respect to infinity (once again, infalling bound gas effectively deposits energy at infinity). It can be decomposed into the gravitational (Eq. 35, blue dashed line) and the kinetic (Eq. 36, blue dotted line) components. Because the flow is only slightly sub-Keplerian and the radial velocities involved are low, these two components behave qualitatively in the same way as in the case of the thin disc discussed in the previous Section.

The magnetic component (Eq. 33), which reflects the energy carried by effective viscosity, also qualitatively agrees with the thin disc prediction. It is zero at the inner edge (which is now at the horizon, not at innermost stable circular orbit (ISCO), because for thick discs stress is not zero down to the horizon), and becomes positive, which again reflects the fact that turbulent viscosity takes energy out of the innermost region (here from $r \lesssim 10$) and carries it outward. In contrast to the thin disc model, however, there is no clear decrease in the magnetic luminosity inside the convergence region of the simulation, i.e., turbulent viscosity does not contribute there to the local heating rate.

Because radiative cooling is not efficient, energy is not transferred by radiation. The dissipated energy is trapped in the flow, heats up the gas, and contributes to the thermal energy transport (Eq. 32). This fact is reflected in the grey line profile in Fig. 4. The luminosity in thermal energy is no longer negligible, as it was in the thin disc case. Significant amount of thermal energy is carried inward with the flow. Because gas becomes hotter when approaching the BH horizon, the corresponding magnitude increases.

If the studied accretion flow followed the standard model, i.e., all the energy released was advected on to the BH, all the components contributing to the energy transfer should sum up to zero total efficiency. This is, however, not the case. The thick red line in Fig. 4 reflects the total luminosity defined through Eq. 29, i.e., composed of binding, magnetic and thermal components. It is flat to a good accuracy inside $r \approx 25$ proving that the flow has reached a quasi-stationary state in this region. The efficiency of $\sim 3\% \dot{M} c^2$, reflects the amount of energy extracted from the accretion flow⁵, and equals roughly 50% of the thin disc efficiency.

In the ideal case of an optically thin disc extending to infinity, this amount of energy would be deposited at infinity. In practice, this is the amount by which the BH systems affects the ISM (the BH

⁵ This value gives the total energy of feedback, in contrast to values given in Sądowski et al. (2013b) who gave only power in jet and wind components.

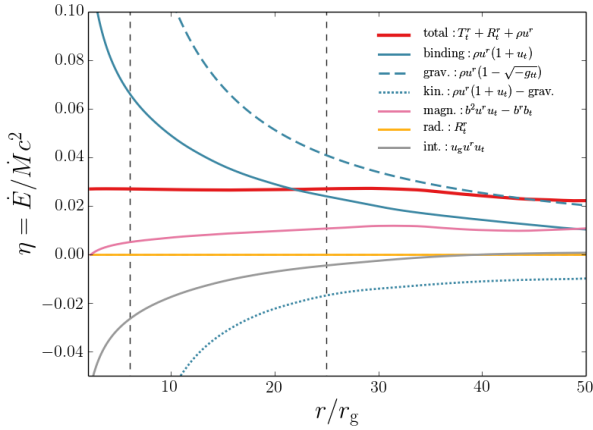


Figure 4. Similar to Fig. 2 but for a GRMHD simulation of an optically thin disc (ADAF, model **h001**). Colors denote the same components of luminosity. Additional gray line reflects the luminosity in thermal (internal) energy. Zero BH spin was assumed. For definitions see Section 3.3. Vertical lines denote the ISCO and the estimated convergence region of the simulation at $r \approx 25$.

feedback). Because simulations with inefficient radiative cooling are scale-free, this efficiency is characteristic of an optically thin flow (ADAF) at *any* accretion rate for which such a solution exists with negligible radiative cooling (i.e., for $\dot{M} \lesssim 10^{-3} \dot{M}$, see Yuan & Narayan 2014). The fate of the energy coming out of the innermost region is discussed below in Section 4.1.

3.3.2 Angular distribution

Figure 5 shows the spatial distribution of density (top-most panel) and various components of the energy flux (other panels) in the optically thin simulation **h001**. The streamlines in the top-most panel reflect the velocity of the gas. The second panel shows the corresponding rest-mass energy flux, ρu^μ . Most of the accretion takes place near the equatorial plane. Within radius $r = 30$, gas at all polar angles falls inward. Only outside this radius (and outside the converged region of the simulation), there is a hint of outflows that may arise from the accretion flow.

The third panel shows the magnitude (colors) and direction on the poloidal plane of the total energy flux, L_{tot} (Eq. 29). The total energy flows outward, in agreement with the positive total efficiency of 3% (see Fig. 4). Most of the extracted energy flows into the disc, and very little in the polar region.

The fourth panel shows the (negative) binding energy brought inward with the gas. This effectively transports energy outward. This component is more isotropic than the net energy flux, reflecting the fact that gas falling in along the axis is more bound than gas accreting in the equatorial plane.

The fifth panel shows the magnetic component, which, as we argued in the previous section, corresponds roughly to the viscous energy transfer rate. As in the case of a thin disc, viscosity transports energy outward and redistributes it throughout the disc. Most of this energy goes near the equatorial plane, where the density is largest, and viscosity most efficient.

Finally, the bottom-most panel presents the flux of internal energy. Its magnitude is significant (compare Fig. 4) because optically thin flow cannot cool efficiently and becomes very hot. As expected, thermal energy is brought inward with the gas, and the angular dis-

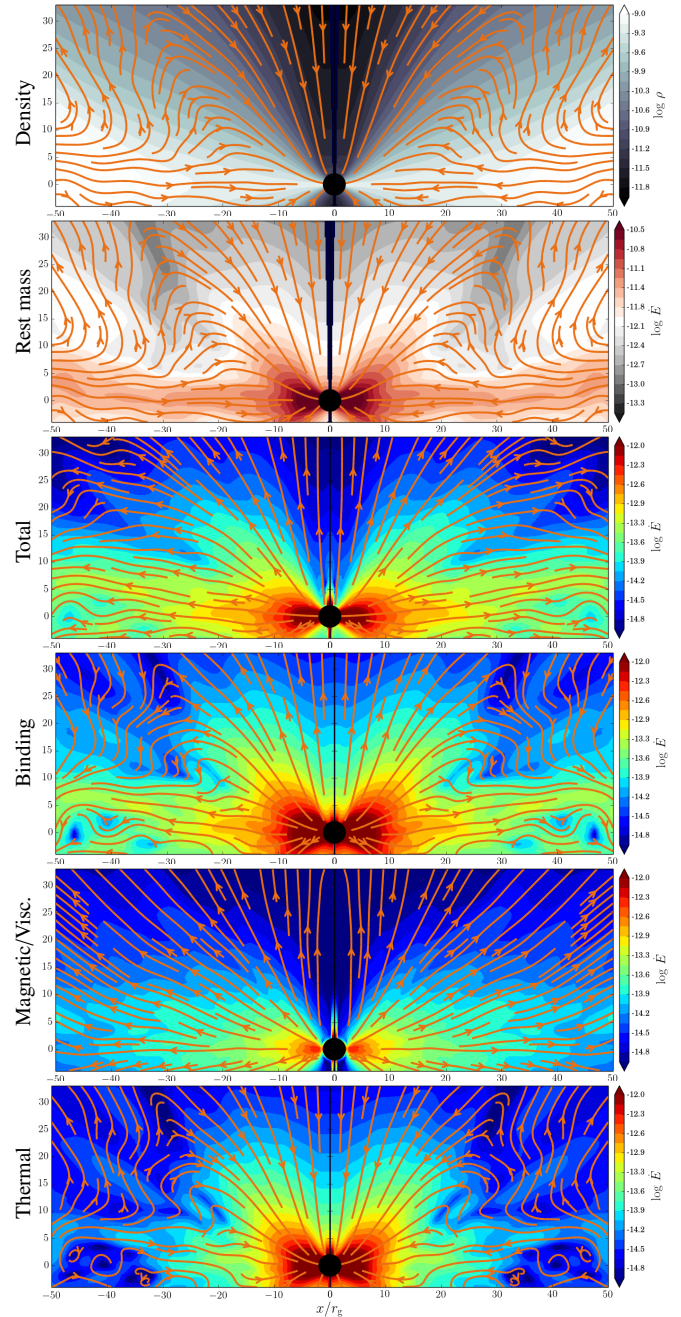


Figure 5. Top panel: Distribution of averaged gas density in optically thin disc (model **h001**). Streamlines reflect direction of average gas velocity. Second panel: Magnitude of the rest mass density flux (colors) and its direction (streamlines). Third to sixth panels: Magnitudes and directions of energy fluxes (total, binding, viscous and Thermal, respectively).

tribution is again quasi-spherical – although the accretion rate is highest near the equatorial plane, the gas temperatures there are lower than in the polar region.

3.4 Energy flow in optically thick super-critical discs

Accretion flows transferring gas at rates higher than the Eddington limit are optically thick, but they are not as radiatively efficient as thin discs. The vertical optical depth is so large, that the cooling time becomes comparable or larger than the accretion time, and

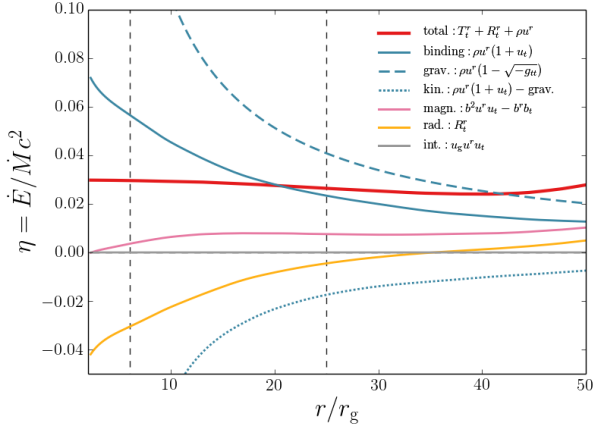


Figure 6. Total luminosity and its components for a GR radiative MHD simulation of optically thick, super-critical disc accreting at $\sim 10\dot{M}_{\text{Edd}}$ on a non-rotating BH (model **r001**). The colors have the same meaning as in Fig. 4.

such discs cannot cool efficiently. Instead, significant fraction of radiation may be advected on to a black hole. We now look closely at the simulation **r001** of a mildly super-critical disc ($10\dot{M}_{\text{Edd}}$) near a non-rotating BH.

3.4.1 Luminosities

Figure 6 shows the luminosities in various components of energy for the super-critical disc **r001**. It can be directly compared to Fig. 4 corresponding to an optically thin disc. The two figures show qualitatively the same behavior of the binding and magnetic components – bound gas is brought inward and effectively transports energy outward, similarly to the magnetic/viscous energy flux which takes energy liberated in the innermost region and redistributes it in the outer regions.

There is, however, a significant difference in the thermal and radiative components. In the case of an optically thin disc, the liberated energy heats up the gas and results in significant inward flux of thermal energy (grey line in Fig. 4). In the case of a radiative super-critical disc, the flux of thermal energy is negligible. Instead, the radiative component is now significant. It is negative within $r \approx 35r_g$, reflecting the fact that photons are trapped in the optically thick flow and transported with the gas to the BH. Only outside this radius, the amount of radiative energy flowing out exceeds the advected one. The fact that the thermal energy is now subdominant with respect to the radiative energy is consistent with the fact that super-critical discs are radiation-pressure dominated, and therefore, inward motion advectively carries radiative energy, not thermal energy.

Interestingly, the total luminosity of the optically thick disc is again close to $3\dot{M}c^2$ (thick red line in Fig. 6). This is the amount of energy returned from the system to the ISM in the case of super-critical accretion on to a non-rotating black hole. Noticeably, the magnitude of BH feedback power from a geometrically thick disc near a non-rotating BH is not sensitive to its optical depth.

3.4.2 Angular distribution

The distribution of the energy fluxes on the poloidal plane for the optically thick simulation **r001** is shown in Fig. 7. The density dis-

tribution (top-most panel) shows much larger contrast between the equatorial plane and the polar axis than in the case of an optically thin disc. This fact results from radiative pressure exerted on the gas in the funnel – gas is accelerated vertically and escapes along the axis. This is clearly reflected in the velocity streamlines shown in that panel.

The total energy extracted from the system (third panel) looks different than in the previous case. This time the polar region is not empty of outflowing energy. The optically thin radiation escaping along the polar funnel dominates the energy budget there.

The distributions of binding and magnetic energy fluxes are similar to the optically thin case. Both transfer energy within the bulk of the disc. For the case of the magnetic energy flux (which reflects the effective viscous transport), this fact supports the conjecture that this energy will dissipate at larger radii (it would not dissipate if the magnetic energy has left the disc, e.g., along the axis).

Finally, the bottom-most panel shows the magnitude and direction of the radiative flux. As already mentioned, radiation manages to escape in the polar region. However, it is trapped in the optically thick flow near the equatorial plane.

3.5 Higher accretion rates

Here, we briefly discuss how the picture described in the previous Section changes when the accretion rate increases but the BH spin remains zero. Detailed comparison of models **r001** (accreting at $10\dot{M}_{\text{Edd}}$) and **r003** ($176\dot{M}_{\text{Edd}}$) was given in Sądowski et al. (2015d). The most important points are as follows.

The total efficiency in both cases equals approximately 3%. However, because of the larger optical depth in model **r003**, photon trapping is more effective. In particular, the polar region becomes optically thick. Inside $r \approx 30$ the gas is dragged on to the BH even along the axis. As a result, radiative luminosity of the system goes down. Fig. 8 shows the fractional contribution of the radiative luminosity, L_{rad} , to the total luminosity L_{tot} . Blue and orange lines correspond to simulations **r001** and **r003**, respectively. It is clear that the latter is less radiatively luminous, and that the effective trapping radius moves outward. This fact, however, turns out not to change the total efficiency.

3.6 Rotating black hole

So far we have been discussing accretion flows around non-rotating BHs. In this Section we briefly discuss what impact non-zero BH spin has on the energy flow properties.

BH spin affects accretion flows in two ways. Firstly, BH rotation modifies the spacetime geometry and for a given BH mass allows for circular orbits getting closer to the horizon with increasing BH spin. This fact results in an increased efficiency of accretion – the closer is the inner edge of the disc, the more binding energy is liberated. Secondly, BH rotational energy can be extracted in the Blandford-Znajek process (Blandford & Znajek 1977). The power of the related jet depends on the value of the BH spin and on the amount of the magnetic flux that has been accumulated at the horizon. The latter is determined by the geometry of the magnetic field in the accreted gas and the efficiency of magnetic field dragging. It is known not to exceed the value characteristic for the magnetically arrested (MAD) state (Igumenshchev et al. 2003; Narayan et al. 2003; Tchekhovskoy et al. 2011).

In this paper we analyze one simulation (**r011**) of super-critical accretion on a mildly-rotating (the non-dimensional spin

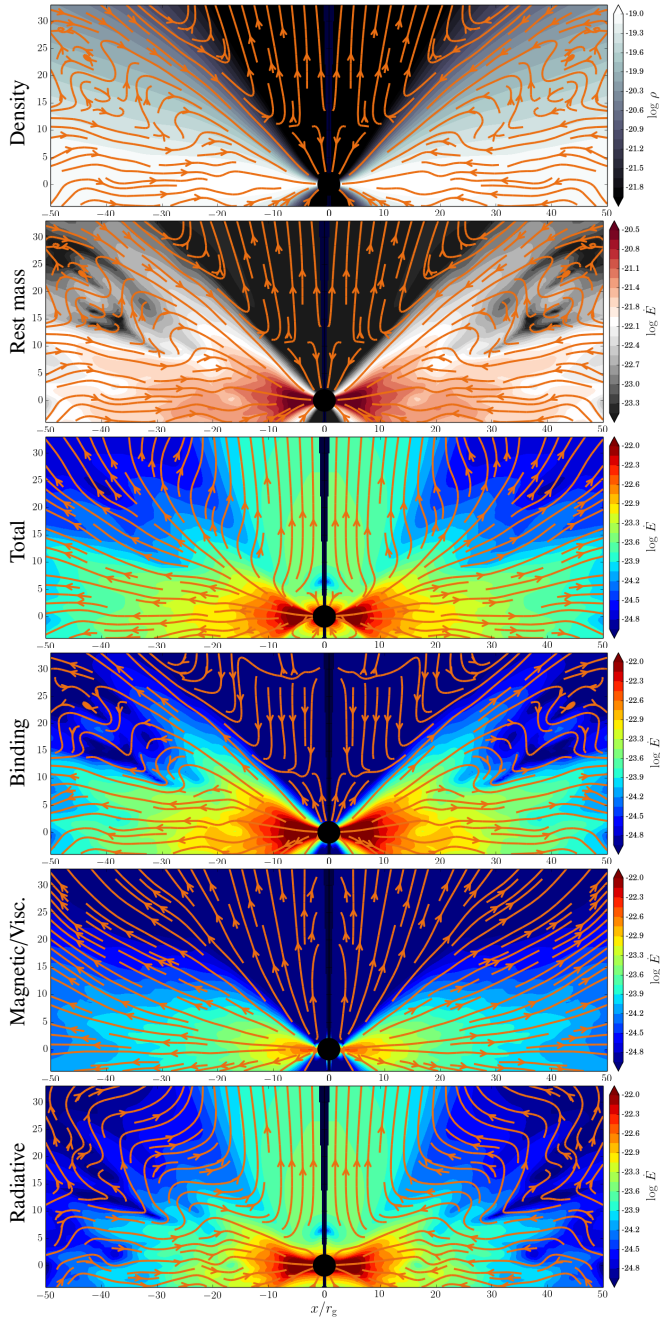


Figure 7. Similar to Fig. 5 but for a super-critical, optically thick disc (model **r001**). The bottom-most panel now shows the flux of energy carried by radiation. The flux of thermal energy is negligible.

parameter $a_* = 0.7$) BH. The average accretion rate in this run ($17\dot{M}_{\text{Edd}}$) is comparable to the fiducial simulation **r001**, and allows for direct comparison. The amount of the magnetic flux accumulated at the BH (the magnetic flux parameter $\Phi \approx 15$) is far from the MAD limit of $\Phi \approx 50$, but is large enough to study the impact of the extracted rotational energy. Optically thick super-critical accretion flows in the MAD limit were studied in a recent work by McKinney et al. (2015).

The total efficiency of simulation **r011** is roughly 8%, significantly higher than that of the comparable simulation on a non-rotating BH (3%). The increase in efficiency comes from both factors mentioned above (modified spacetime geometry and the ex-

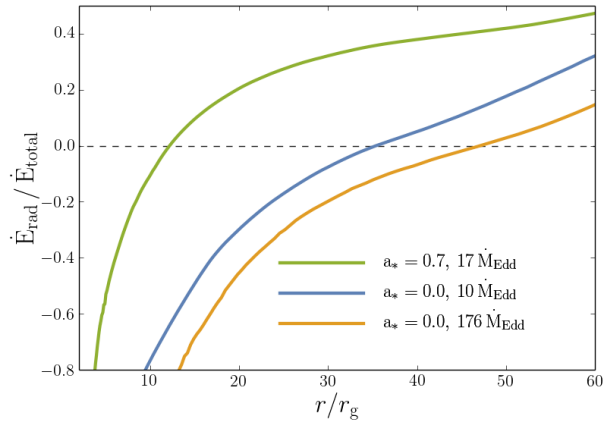


Figure 8. Fractional contribution of the radiative luminosity to the total luminosity in simulations **r011** (green), **r001** (blue), **r003** (orange lines). The luminosities were obtained by integrating corresponding fluxes over the whole sphere. The radiative luminosity, in particular, includes both the radiation trapped in the flow and escaping to infinity.

traction of the rotational energy). The latter by itself should extract $\sim 6\% \dot{M}c^2$ for the accumulated amount of magnetic flux and spin $a_* = 0.7$, but decomposition of the total energy into these two components is not straightforward.

In Fig. 9 we show the distribution of energy flux components on the poloidal plane. The panels have the same meaning as in the previously discussed Fig. 7. There are a couple of noticeable differences between the two. Most importantly, the amount of total energy extracted into the funnel region is much higher for the rotating BH case. This is expected, because the energy extracted in the Blandford-Znajek is known to go roughly along the axis (Penna et al. 2013c). In the case of optically thin accretion on a rotating BH (e.g., Tchekhovskoy & McKinney 2012; Sądowski et al. 2013b), the jet power is extracted as magnetic Poynting flux gradually converting (if mass loading is significant) into kinetic energy of gas. In the case of the radiative flow studied here, this extra energy is carried mostly by radiation already for $r \gtrsim 3r_g$. Magnetic flux is significant only in a shell surrounding the funnel region. Fig. 10 shows the magnitude and direction of the radiative flux in the immediate vicinity of the BH. As expected, radiative flux falls *on the BH* in this innermost region, and it is the magnetic energy which is extracted at the horizon. However, the latter is quickly converted into the radiative energy. This is possible because the magnetic field efficiently pushes hot and optically thick gas along the axis. The gas, in turn, drags the radiation upward.

At the risk of oversimplifying, it is possible to say that the properties of an energy flow in the case of a super-critical accretion on a rotating BH are a superposition of the disk component (discussed in Section 3.4 for a non-rotating BH) and the jet contribution coming from the Blandford-Znajek process. The power of the latter depends on the BH spin and magnetic flux threading the horizon, and may overwhelm the former in magnitude. At the same time, the jet component is limited only to the polar region. If the confinement provided by the disc is strong enough, it is likely to stay collimated.

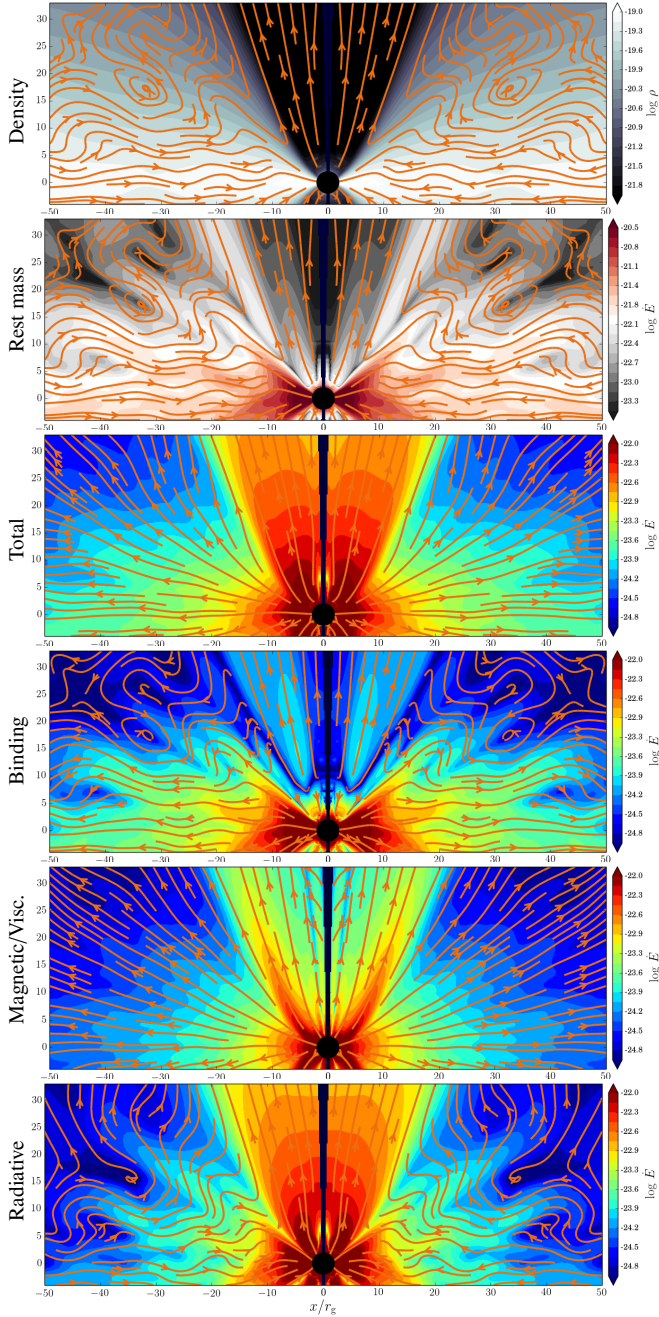


Figure 9. Similar to Fig. 7 but for a model with spinning BH (model r011).

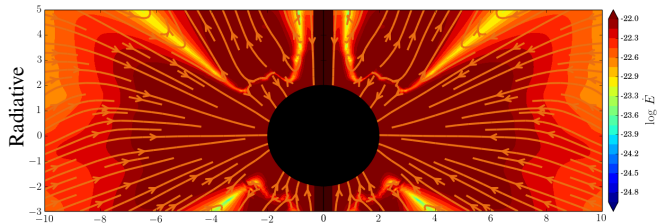


Figure 10. Zoomed in magnitude and direction of radiative energy flux for a model with spinning BH (model r011).

4 DISCUSSION

4.1 The fate of the energy flow

We have shown so far that in geometrically thick discs, both optically thin and thick, a significant flux of energy is liberated in the accretion flow and flows out of the system. Although the simulations we performed allowed us to study only the innermost ($r \lesssim 25$ at the equatorial plane) region of the flow⁶, we were able to infer the total luminosity of the system. This is because in a stationary state this quantity is determined by the energy flux crossing the BH horizon.

However, the adopted method does not allow to study what happens to the extracted energy outside the inflow/outflow equilibrium region (i.e., for $r \gtrsim 25$) – only for gas inside this region the duration of the simulations was longer than the viscous time scale.

As Figs. 4 and 6 show, the total luminosity of the flows around a non-rotating BH (roughly $3\%Mc^2$) comprises three components at radius $r = 25$. The largest in the magnitude is the binding energy flux which effectively deposits energy at infinity. The magnetic component (reflecting the viscous energy transport) is also transporting energy outward in a significant amount. The remainder goes either into the thermal (for optically thin case) or radiative energy (for optically thick) component. In both cases their net effect results in advecting energy inward.

The binding energy consists of the gravitational and kinetic components (plotted with dashed and dotted blue lines, respectively, in Figs. 4 and 6). The former goes to zero with increasing radius, and *at infinity* no gravitational energy is transported by the gas. The kinetic component is negative inside the computational domain reflecting the fact that gas flows inward and carries kinetic energy of its rotational motion. However, when outflows are efficiently generated it might become ultimately positive outside the computational domain.

As we have shown above, the radial flux of magnetic energy reflects the effective viscous energy transfer. Viscosity not only transports angular momentum and energy, but also leads to dissipation of the latter. Therefore, one may expect that the amount of energy carried by magnetic fields will dissipate sooner or later outside the convergence region of the simulation, adding up to the local heating rate in the same way as for thin discs discussed in Section 2. Thus, no magnetic energy will be ultimately directly deposited in the ISM.

The radiative energy transfer is important only for optically thick accretion flows. Simulations of such flows described in this paper (models r001 and r003) show significant photon trapping in the bulk of the disc which results in negative net flow of radiative energy (see Figs. 6 and 8) in the inner region. However, as radiation gradually diffuses out from the disc, the outflowing component finally overcomes inward advection, and the net radiative luminosity becomes positive. In particular, from the point of view of an observer at infinity, radiation will only carry energy outward. In the following Section we discuss how bright the accretion flow can be.

The thermal energy flux, which contributes significantly to the energy transfer rate in optically thin accretion flows, reflects both the advective and convective contributions. In the inner part of the flow it is the advective component which dominates and results in

⁶ Obtaining an equilibrium solution in a larger domain is computationally very demanding because of the increasing range of timescales. An appropriate approach would be to divide the domain into subregions which are simulated independently but coupled at the boundaries (e.g. Yuan et al. 2012).

negative net energy transfer rate – hot gas is accreted and takes its thermal energy with it. However, if outflows are present in the outer region, the net effect may be opposite and the thermal energy carried advectively outward with the outflowing gas may dominate.

Convection can carry energy against the gravity without transporting mass. This component is negligible in the simulations we performed (thermal energy flows advectively inward), but in principle it may become significant, or even dominant, in the outer region. Several models of accretion flows which are dominated by convection (convectively dominated accretion flows, CDAFs) have been formulated (Quataert & Gruzinov 2000; Narayan et al. 2000, 2002; Abramowicz et al. 2002). Whether convection is important is an open question. Narayan et al. (2012) performed a set of simulations similar to our model h001 and showed that optically thin flows are convectively stable within $r \lesssim 100$. On the other hand, Yuan et al. (2015), who studied non-magnetized viscous flows on large scales, found that the accretion flow is actually convectively unstable. Even if convection is important, it cannot transport energy beyond the outer edge of the disc (or beyond the Bondi radius). One may expect that ultimately all energy transported by convection is released as radiation or generates outflow.

To sum up, geometrically thick accretion flows on to a non-rotating BHs deposit in the ISM roughly 3% of the rest-mass energy crossing the BH horizon. This energy may be transported outward with the outflowing gas, radiation and convection. Which components dominate is currently unclear. Ultimately, however, only radiation and outflow can transport energy beyond the Bondi radius and deposit it in the ISM. A separate jet component may be present in case of a spinning BH which managed to accumulate significant magnetic flux at its horizon. It will result in a collimated, narrow outflow of mostly kinetic energy, unlikely to interact efficiently with the ISM.

4.2 Radiative luminosity

Radiation is one of the ways of extracting energy from accretion flows. The total luminosity (accounting for all forms of energy) for a thick disc near a non-rotating BH seems to be robust – every simulation we have performed indicates that roughly 3% of the accreted rest-mass energy is returned to ISM. The amount of this energy that goes into radiation is not, however, easy to estimate. Only when the photosphere is properly resolved, one can check if radiation reaches the observer at infinity. This is not the case for any of the optically thick simulations discussed here. They were run only for a time which allowed them to reach inflow/outflow equilibrium state at the equatorial plane within $r \approx 25$. Because of large optical depths, photospheres are located at large distances (Sądowski et al. 2015a), significantly outside the converged region. This fact makes it impossible to directly measure the amount of radiation escaping the system. Only radiation escaping along optically thin funnel, if it exists, is guaranteed to reach a distant observer.

Because of significant photon trapping in the super-Eddington regime, the radiative luminosity of the system is not proportional to the accretion rate. What is more, the radiation coming from such an accretion flow must penetrate the optically thick wind region. It cannot be therefore locally significantly super-Eddington, because in such a case it would transfer its energy and momentum to the gas accelerating it. We are inclined to suggest that the result will be similar to the effect of pure photon trapping which results in logarithmic dependence of the luminosity on the accretion rate (already anticipated by Shakura & Sunyaev (1973), see also Begelman

(1979)),

$$L_{\text{rad}} \approx L_{\text{Edd}} \left(1 + \log \dot{M} / \dot{M}_{\text{Edd}}\right). \quad (40)$$

A similar logarithmic behavior was found in the old works on super-Eddington Polish Doughnuts and explained by Paczynski and collaborators as being a consequence of the drop in efficiency when, with increasing accretion rate, the inner edge of the accretion disc moves from the ISCO to the innermost bound circular orbit (IBCO), where the efficiency is zero (see Wielgus et al. 2015, for explanation and references).

4.3 Outflow

Our work shows that the existence of outflows is inevitable in outer parts of thick accretion discs. Avoiding them requires *all* of the extracted energy to be ultimately transported outwards by radiation. However, thick discs are radiatively inefficient (see Eq. 40).

This conclusion is based on disc energetics – a significant fraction of the accreted rest mass energy flows outward through the disc which cannot generate enough radiation to provide the efficient cooling required to get rid of the energy surplus. If convection is not effective, at least in the outermost region, outflow is the only possible way of taking this excess of energy out of the system.

We do not see strong outflows in the simulations we performed (compare topmost panels in Figs. 5, 7, and 9). Only in the funnel region of optically thick simulations r003 and r011 one observes that the radiative luminosity is converted gradually into kinetic energy of the outflowing gas. However, the kinetic luminosity of such gas measured at the outer boundary is still at most $\sim 10\%$ of the total efficiency.

Therefore, one may expect that most of the outflow will be generated at radii larger than covered by the inflow/outflow equilibrium region of the simulations, i.e., at $r \gtrsim 25r_g$. What will drive these outflows? In principle, there are three acceleration mechanisms likely to act in magnetized accretion flows – magnetocentrifugal (Blandford & Payne 1982), radiative and thermal. Magnetocentrifugal driving is not effective in the simulated inner region of a non-MAD accretion flow (see also Möller & Sądowski 2015), and there is little hope for it to become effective further out, where magnetic field has no reason to be more uniform on large scales. Radiative driving is seen in the funnel region of the simulated super-critical discs, but does not result in significant outflow at larger polar angles – radiation diffusing out of the disc into the optically thick wind region is supporting the disc against gravity, and therefore cannot on average significantly exceed the local Eddington flux.

Thermal wind driving remains the only candidate to balance the energy budget of the discs. It is especially reasonable if we consider the energy flux redistributed through viscosity. When it finally dissipates at larger radii, it will heat up the gas and make it more prone to become unbound and likely to flow out of the system. This is in agreement with the standard ADAF model which predicts positive Bernoulli function for the inflowing gas in the self-similar regime (Narayan & Yi 1994). At the same time, most of the observed outflows in BH accretion flows are believed to be of thermal nature (e.g., Lee et al. 2002; Ponti et al. 2012; Neilsen 2013).

The total luminosity will be ultimately carried by the outflow and radiation. Thus, at infinity, the outflow will carry the amount of energy equal to the difference between the total and radiative luminosities. For a non-spinning BH one will have,

$$L_{\text{outflow},\infty} = 0.03\dot{M}c^2 - L_{\text{rad},\infty}. \quad (41)$$

The latter term is obviously negligible for optically thin discs, for which the whole extracted energy goes into outflow.

4.4 Extent of a thick disc

In the considerations so far we assumed that the accretion flow extends to infinity, and that the gas at infinity has negligible energy, i.e., its Bernoulli number is zero. These conditions do not have to be satisfied in reality. In particular, a thick disc is expected to become thin in the outer region. For example, a super-critical disc becomes radiatively efficient at a sufficiently large radius where its optical depth is no longer large enough to prevent locally generated radiation from diffusing out in an efficient way. Somewhat similarly, optically thin discs (ADAFs) cannot exist above a critical accretion rate, and this limit decreases with radius. Therefore, for a fixed accretion rate at a BH, there is a radius where thick disc must become thin, and radiatively efficient. In such cases, the picture presented here would have to be modified accordingly, e.g., if at the transition radius the outward energy flux inside the disc (i.e., not in the outflow) is still significant, then one could expect that the thin disc, extending from this radius outward, will ultimately release all its energy as (relatively cold) radiation.

4.5 Transition between accretion modes

We did not simulate thin, sub-Eddington accretion flows, for which the standard assumption of being radiatively efficient is satisfied by construction. For such discs, the energy transfer is expected to follow the characteristics described in Section 2, i.e., the total efficiency of BH feedback equals the thin disc efficiency, and ultimately all of it is carried by radiation which is emitted over a wide solid angle. Geometrically thin discs are unlikely to drag significant amount of magnetic field on to the BH (e.g., Lubow et al. (1994), Ghosh & Abramowicz (1997), Guilet & Ogilvie (2012, 2013), but see also Spruit & Uzdensky (2005), Rothstein & Lovelace (2008) and Beckwith et al. (2009)) and therefore one does not expect strong Blandford-Znajek jet component.

The transition between optically thick but geometrically thin and thick discs takes place near the Eddington accretion rate. In the past it has been modeled with the so called slim disc model (e.g., Abramowicz et al. 1988; Sądowski 2011) which generalizes the standard thin disc model to higher accretion rates. Recently, numerical simulations similar to the ones that this work is based on, have studied a number of super-Eddington accretion flows (e.g., Sądowski et al. 2015a; Jiang et al. 2014b). Simulations of thin discs, more demanding computationally, have not yet been performed. Below, we will describe the transition between geometrically thin and thick optically thick discs with the help of arbitrary step functions, which make the final formulae agree qualitatively with what we have learned from numerical, multi-dimensional simulations.

The transition between optically thin and thick discs is even less well understood and awaits numerical modeling. It is known that radiatively inefficient optically thin flows cannot exist above some critical accretion rate $\dot{M}_{\text{ADAF}} \approx 10^{-3} \dot{M}_{\text{Edd}}$ (e.g., Esin et al. 1997). Whether increasing the accretion rate above this threshold results in a dramatic transition to a cold, optically thick disc, or rather the disc takes a form similar to the luminous-hot accretion flow (LHAF, Yuan 2001), has still to be verified.

Below, for simplicity, we assume that whenever accretion rate is below \dot{M}_{ADAF} , accretion occurs in optically thin disc, and that

the transition to optically thick discs (for $\dot{M} > \dot{M}_{\text{ADAF}}$) takes place instantaneously.

Having these considerations in mind, one may approximate the total amount of feedback luminosity coming from an accreting system as,

$$L_{\text{fb}} = \frac{1}{2} \eta_{\text{thin}} \dot{M} c^2 + P_{\text{BZ}}, \quad (42)$$

for $\dot{M} < \dot{M}_{\text{ADAF}}$ (opt. thin),

$$L_{\text{fb}} = \eta_{\text{thin}} \left(1 - \frac{1}{2} f_{\eta} \right) \dot{M} c^2 + f_{\text{BZ}} P_{\text{BZ}}, \quad (43)$$

for $\dot{M} > \dot{M}_{\text{ADAF}}$ (opt. thick),

where η_{thin} stands for the efficiency of a standard thin disc with given spin, the 1/2 factor reflects two times smaller efficiency of thick discs, and where we allow for the Blandford-Znajek contribution, P_{BZ} , for thick discs. $\dot{M}_{\text{ADAF}} \approx 10^{-3} \dot{M}_{\text{Edd}}$ is the critical accretion rate above which radiatively inefficient optically thin accretion flows do not exist. Functions f_{η} and f_{BZ} ,

$$f_{\eta} = \left(1 + \left(\frac{3}{\dot{M}/\dot{M}_{\text{Edd}}} \right)^3 \right)^{-1} \quad (44)$$

$$f_{\text{BZ}} = \left(1 + \left(\frac{1}{\dot{M}/\dot{M}_{\text{Edd}}} \right)^5 \right)^{-1} \quad (45)$$

were chosen to give (arbitrary) smooth transitions between the sub- and super-Eddington regime for the efficiency and the jet power, respectively. The Blandford-Znajek term (given here for saturated magnetic field at the BH, i.e., for the MAD limit, see Tchekhovskoy 2015),

$$P_{\text{BZ}} = 1.3 a_*^2 \dot{M} c^2, \quad (46)$$

is strongly damped for thin discs which are not likely to drag the magnetic fields effectively.

Fig. 11 shows the disc and jet components of the total black hole feedback, L_{fb} (Eqs. 42 & 43), as a function of accretion rate for BH spins $a_* = 0.0$ and 0.7. For the latter, we assumed that magnetic field saturated at the BH at half of the MAD limit (in this way the jet power was not overwhelming the power of the disc component).

The solid lines show the efficiency of the feedback coming from the disc. In the thin disc regime ($\dot{M}_{\text{ADAF}} \lesssim \dot{M} \lesssim \dot{M}_{\text{Edd}}$), this efficiency equals the standard thin disc efficiency - $\eta = 0.057$ and 0.104 for $a_* = 0.0$ and 0.7, respectively. For accretion rates significantly exceeding the Eddington limit, this efficiency drops down to roughly half of the thin disc efficiency, i.e., to $\eta = 0.03$ for a non-rotating BH. The proposed formulae make the transition between the two regimes smooth. In the limit of low accretion rates $\dot{M} < \dot{M}_{\text{ADAF}}$, one expect accretion flows to be optically thin with similar efficiency of $\eta = 0.03$. The transition to the thin disc limit is probably more violent, and we did not apply any smoothing function there.

The dashed lines reflect the power of the jet feedback component. It is non-zero only for the case of a rotating BH. For geometrically thick discs jet production is efficient and given (for magnetic flux at the BH saturated at half of the MAD limit) by $1/4 P_{\text{BZ}}$ (see Eq. 46). Thin discs are unlikely to provide strong jet components and therefore we damp the jet power in this regime. One has to keep in mind that the jet component will be highly collimated and may not interact efficiently with the ISM.

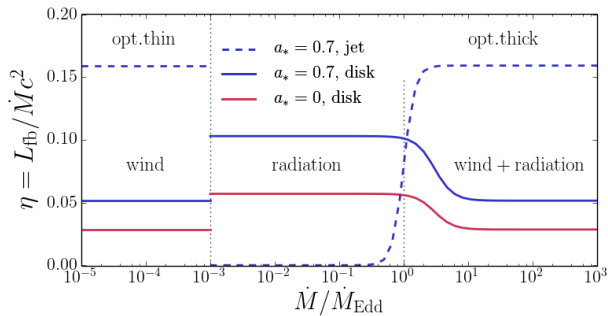


Figure 11. Total efficiency of the feedback (Eqs. 42 & 43) for $a_* = 0.0$ (red) and 0.7 (blue lines) BHs. Solid and dashed lines represent the disc and jet components, respectively. The jet component was calculated assuming magnetic field saturation at half the MAD limit. $\dot{M}_{\text{ADAF}} = 10^{-3} \dot{M}_{\text{Edd}}$ is an estimated transition between optically thin and thick accretion flows.

5 SUMMARY

In this paper we have studied the flow of energy in geometrically thick discs, both optically thin and thick. We based our study on a set of state-of-the-art, three-dimensional simulations of accretion flows performed in the framework of general relativity. Our results are as follows:

(i) *Total feedback:* Thick accretion flows on a non-rotating BH show the same total efficiency of $3\% \dot{M} c^2$ (roughly 50% of the thin disc efficiency) independent of the accretion rate. Both optically thin, ADAF-like flows, and super-Eddington optically thick flows liberate energy at the same rate. This energy is ultimately distributed between the energy carried by outflow and radiation. The efficiency of accretion flows onto a rotating BH is increased by the modified spacetime geometry and the rate at which BH rotational energy is extracted through the Blandford-Znajek process.

(ii) *Approximated formulae:* One may approximate the total amount of feedback coming from an accreting system using Eqs. 42 and 43. These formulae assume that the total efficiency of the feedback disc component, i.e., the amount of energy extracted from the disc itself, and not from the jet, equals half of the thin disc efficiency for geometrically thick discs, as found in this work.

(iii) *Energy in the outflow:* The energy outflowing from the system can be ultimately carried away only by radiation or outflowing gas. If a disc cannot cool efficiently, i.e., if it is not luminous (in radiation), then most of the liberated energy must be carried by the outflow. This is true both for optically thin discs and for optically thick discs which at sufficiently high accretion rates efficiently trap radiation in the gas. Therefore, we can infer the existence of outflows even if they are not emerging strongly within the computational domain.

The amount of energy, either kinetic or thermal, carried by the outflow equals,

$$L_{\text{outflow}} = L_{\text{fb}} - L_{\text{rad}}, \quad (47)$$

where the radiative luminosity is zero for optically thin discs and may be approximated as,

$$L_{\text{rad}} \approx L_{\text{Edd}} \left(1 + \log \dot{M} / \dot{M}_{\text{Edd}} \right), \quad (48)$$

for super-critical discs.

(iv) *Outflowing mass:* Our study is based on simulations covering only the innermost region of BH accretion. We find that significant amount of energy flows out from that region and likely results in outflowing mass from larger radii. However, despite the fact

that we know how energetic the outflow can be, we are not able to say in what amount gas is blown away. The relation between the two depends on the Bernoulli function of the outflowing gas, e.g., marginally bound gas will carry virtually zero energy per unit mass. Because of similar reasons we cannot determine the amount of momentum carried with the outflow. As Begelman (2012) points out, accretion through thick, advective discs leads to either winds or breezes. To find how much gas is lost on the way towards the BH, one has to solve the problem consistently on larger scales than covered by the simulations presented here. Recently, a significant progress in this direction has been made by Yuan et al. (2015) and Bu et al. (2015), who studied optically thin accretion flows and found that gas is likely lost between $r \approx 40$ and the Bondi radius, and that the mass loss rate in the wind increases proportionally to radius according to $\dot{M}_{\text{out}} = \dot{M}_{\text{BH}}(r/40)$.

(v) *Angular distribution of feedback:* In the case of optically thin accretion, the liberated energy can flow out in two channels. The jet component related to the extraction of BH rotational energy is collimated along the axis and ultimately results in a narrow, relativistic magnetized jet. The accretion component flows outward in the bulk of the disc and is responsible for driving the outflows at large radii or ultimately leaves the system in convective eddies. Such energy flows will have a quasi-spherical distribution in space and will likely interact efficiently with ISM.

To some extent similar properties characterize outflows in case of super-critical, optically thick discs. The jet component is likely to be collimated along the axis, while the outflow component covers wide range of angles. The radiation coming out of the system may have initially a mildly collimated component in the funnel region (the radiative jet, see Sądowski et al. 2015b). However, it either converts into kinetic jet (if there is enough coupling between radiation and gas in the funnel), or ultimately diffuses when the funnel opens because of only mild collimation of the photon beams (Jiang et al. 2014b; Narayan et al. 2015). Therefore, the radiation component should be expected to cover large solid angle from the point of view of a distant observer. Thin accretion discs, which we did not study here, are expected to produce largely isotropic radiative feedback.

(vi) *Models of thick discs:* Our study shows that outflows in some form or convection is inevitable for thick discs. This is not surprising because advection dominated accretion involve fluid which is only weakly bound to the BH (Narayan & Yi 1994; Blandford & Begelman 1999). Existence of outflows or convection in principle rules out well known and celebrated models of thick accretion flows which assume that gas is not lost on the way towards the BH, and which do not allow for convection, i.e., optically thick slim discs (Abramowicz et al. 1988) and optically thin ADAFs (Narayan & Yi 1994; Abramowicz et al. 1995). However, the outflow and convective regions do not extend all the way down to the BH. Therefore, the innermost region *can* be described with the use of these models.

In the outer region the situation is less clear because all the proposed semi-analytic models for convection and winds suffer from some problems, or they have been developed, as the recent inflow-outflow solution by Begelman (2012), in application for the inner part of the flow. In particular, the models of convectively dominated discs (Quataert & Gruzinov 2000; Narayan et al. 2000, 2002; Abramowicz et al. 2002) in optically thin flows are self-similar. The Dotan & Shaviv (2011) model for slim discs with winds uses sophisticated descriptions of the disc and the wind separately, but assumes an ad hoc wind launching mechanism. Finally, simple and widely used ADIOS model (Blandford & Begelman 1999) takes

strong assumptions which have been criticized by Abramowicz et al. (2000).

6 ACKNOWLEDGEMENTS

AS acknowledges support for this work by NASA through Einstein Postdoctoral Fellowship number PF4-150126 awarded by the Chandra X-ray Center, which is operated by the Smithsonian Astrophysical Observatory for NASA under contract NAS8-03060. AS thanks Harvard-Smithsonian Center for Astrophysics for its hospitality. This research was supported by the Polish NCN grants UMO-2013/08/A/ST9/00795 and DEC-2012/04/A/ST9/00083. JPL was supported in part by a grant from the French Space Agency CNES. RN was supported in part by NSF grant AST1312651 and NASA grant TCAN NNX14AB47G. The authors acknowledge computational support from NSF via XSEDE resources (grant TG-AST080026N), and from NASA via the High-End Computing (HEC) Program through the NASA Advanced Supercomputing (NAS) Division at Ames Research Center.

REFERENCES

- Abramowicz, M. A., Czerny, B., Lasota, J. P., & Szuszkiewicz, E. 1988, *Astrophysical Journal*, 332, 646
- Abramowicz, M. A., Chen, X., Kato, S., Lasota, J.-P., & Regev, O. 1995, *Astrophysical Journal Letters*, 438, L37
- Abramowicz, M. A., Lasota, J.-P., & Igumenshchev, I. V. 2000, *Monthly Notices of the Royal Astronomical Society*, 314, 775
- Abramowicz, M. A., Igumenshchev, I. V., Quataert, E., & Narayan, R. 2002, *Astrophysical Journal*, 565, 1101
- Beckwith, K., Hawley, J. F., & Krolik, J. H. 2009, *Astrophysical Journal*, 707, 428
- Begelman, M. C. 1979, *Monthly Notices of the Royal Astronomical Society*, 187, 237
- Begelman, M. C. 2012, *Monthly Notices of the Royal Astronomical Society*, 420, 2912
- Blandford, R. D., & Begelman, M. C. 1999, *Monthly Notices of the Royal Astronomical Society*, 303, L1
- Blandford R. D., Payne D. G., 1982, *MNRAS*, 199, 883
- Blandford R. D., Znajek R. L., 1977, *MNRAS*, 179, 433
- Bu, D.-F., Yuan, F., Gan, Z.-M., Yang, X.-H. 2015, *astro-ph/1510.03124*
- Cowie, L. L., & Binney, J. 1977, *Astrophysical Journal*, 215, 723
- Croton, D. J., Springel, V., White, S. D. M., et al. 2006, *Monthly Notices of the Royal Astronomical Society*, 365, 11
- Dotan, C., & Shaviv, N. J. 2011, *Monthly Notices of the Royal Astronomical Society*, 413, 1623
- Esin, A. A., McClintock, J. E., & Narayan, R. 1997, *Astrophysical Journal*, 489, 865
- Fabian, A. C., & Nulsen, P. E. J. 1977, *Monthly Notices of the Royal Astronomical Society*, 180, 479
- Fabian, A. C., Churazov, E., Donahue, M., et al. 2009, *astro2010: The Astronomy and Astrophysics Decadal Survey*, 2010, 73
- Frank, J., King, A., & Raine, D. 1992, *Camb. Astrophys. Ser.*, Vol. 21
- Gammie, C. F., McKinney, J. C., & Tóth, G. 2003, *Astrophysical Journal*, 589, 444
- Ghosh, P., & Abramowicz, M. A. 1997, *Monthly Notices of the Royal Astronomical Society*, 292, 887
- Guilet, J., & Ogilvie, G. I. 2012, *Monthly Notices of the Royal Astronomical Society*, 424, 2097
- Guilet, J., & Ogilvie, G. I. 2013, *Monthly Notices of the Royal Astronomical Society*, 430, 822
- Hopkins, P. F., Kereš, D., Oñorbe, J., et al. 2014, *Monthly Notices of the Royal Astronomical Society*, 445, 581
- Igumenshchev, I. V., Narayan, R., & Abramowicz, M. A. 2003, *Astrophysical Journal*, 592, 1042
- Jiang, Y.-F., Stone, J. M., & Davis, S. W. 2012, *Astrophysical Journal Suppl. Ser.*, 199, 14
- Jiang, Y.-F., Stone, J. M., & Davis, S. W. 2014, *Astrophysical Journal Suppl. Ser.*, 213, 7
- Jiang, Y.-F., Stone, J. M., & Davis, S. W. 2014, *Astrophysical Journal*, 796, 106
- Komissarov, S. S. 1999, *Monthly Notices of the Royal Astronomical Society*, 303, 343
- Lee, J. C., Reynolds, C. S., Remillard, R., et al. 2002, *Astrophysical Journal*, 567, 1102
- Levermore, C. D. 1984, *Journal of Quantitative Spectroscopy and Radiative Transfer*, 31, 149 2
- Lubow, S. H., Papaloizou, J. C. B., & Pringle, J. E. 1994, *Monthly Notices of the Royal Astronomical Society*, 267, 235
- McKinney, J. C., Dai, L., & Avara, M. J. 2015, *Monthly Notices of the Royal Astronomical Society*, 454, L6
- Möller, A., Sądowski, A. 2015, in prep
- Narayan, R., & Yi, I. 1994, *Astrophysical Journal Letters*, 428, L13
- Narayan, R., Igumenshchev, I. V., & Abramowicz, M. A. 2000, *Astrophysical Journal*, 539, 798
- Narayan, R., Quataert, E., Igumenshchev, I. V., & Abramowicz, M. A. 2002, *Astrophysical Journal*, 577, 295
- Narayan, R., Igumenshchev, I. V., & Abramowicz, M. A. 2003, *Publications of the Astronomical Society of Japan*, 55, L69
- Narayan, R., Sądowski, A., Penna, R. F., & Kulkarni, A. K. 2012, *Monthly Notices of the Royal Astronomical Society*, 426, 3241
- Narayan, R., Zhu, Y., Psaltis, D., & Sądowski, A. 2015, *MNRAS submitted*, arXiv:1510.04208
- Neilsen, J. 2013, *Advances in Space Research*, 52, 732
- Novikov, I. D., & Thorne, K. S. 1973, *Black Holes (Les Astres Occlus)*, 343
- Ohsuga, K., & Mineshige, S. 2007, *Astrophysical Journal*, 670, 1283
- Ohsuga, K., Mineshige, S., Mori, M., & Yoshiaki, K. 2009, *Publications of the Astronomical Society of Japan*, 61, L7
- Ohsuga, K., & Mineshige, S. 2011, *Astrophysical Journal*, 736, 2
- Ohsuga, K., & Takahashi, H. R. 2015, *Astrophysical Journal*, submitted Paczyński, B. 2000, arXiv:astro-ph/0004129
- Penna, R. F., Kulkarni, A., & Narayan, R. 2013a, *Astronomy & Astrophysics*, 559, A116
- Penna, R. F., Sądowski, A., Kulkarni, A. K., & Narayan, R. 2013a, *Monthly Notices of the Royal Astronomical Society*, 428, 2255
- Penna, R. F., Narayan, R., & Sądowski, A. 2013c, *Monthly Notices of the Royal Astronomical Society*, 436, 3741
- Pessah, M. E., Chan, C.-K., & Psaltis, D. 2006, *Monthly Notices of the Royal Astronomical Society*, 372, 183
- Ponti, G., Fender, R. P., Begelman, M. C., et al. 2012, *MNRAS*, 422, L11
- Quataert, E., & Gruzinov, A. 2000, *Astrophysical Journal*, 539, 809
- Rothstein, D. M., & Lovelace, R. V. E. 2008, *Astrophysical Journal*, 677, 1221
- Sądowski, A. 2011, Ph.D. Thesis, Nicolaus Copernicus Astronomical Center, Polish Academy of Sciences, arXiv:1108.0396
- Sądowski, A., Narayan, R., Tchekhovskoy, A., & Zhu, Y. 2013a, *Monthly Notices of the Royal Astronomical Society*, 429, 3533
- Sądowski, A., Narayan, R., Penna, R., & Zhu, Y. 2013b, *Monthly Notices of the Royal Astronomical Society*, 436, 3856
- Sądowski, A., Narayan, R., McKinney, J. C., & Tchekhovskoy, A. 2014, *Monthly Notices of the Royal Astronomical Society*, 439, 503
- Sądowski, A., Narayan, R., Tchekhovskoy, A., Abarca, D., Zhu, Y., & McKinney J. C. . 2015a, *Monthly Notices of the Royal Astronomical Society*, 447, 49
- Sądowski, A., & Narayan, R. 2015b, *Monthly Notices of the Royal Astronomical Society*, 453, 3213
- Sądowski, A., & Narayan, R. 2015c, *Monthly Notices of the Royal Astronomical Society*, 454, 2372
- Sądowski, A., & Narayan, R. 2015d, *MNRAS*, submitted, arXiv:1509.03168

- Shafee, R., McKinney, J. C., Narayan, R., et al. 2008, *Astrophysical Journal Letters*, 687, L25
- Shakura, N. I., & Sunyaev, R. A. 1973, *A&A*, 24, 337
- Spruit, H. C., & Uzdensky, D. A. 2005, *Astrophysical Journal*, 629, 960
- Tchekhovskoy, A., Narayan, R., & McKinney, J. C. 2011, *Monthly Notices of the Royal Astronomical Society*, 418, L79
- Tchekhovskoy, A., & McKinney, J. C. 2012a, *Monthly Notices of the Royal Astronomical Society*, 423, L55
- Tchekhovskoy, A. 2015, *Astrophysics and Space Science Library*, 414, 45
- Tóth, G. 2000, *Journal of Computational Physics*, 161, 605
- Wielgus M., J.-P. Lasota, Yan W., Abramowicz M.A. 2015, in preparation
- Yuan, F. 2001, *Monthly Notices of the Royal Astronomical Society*, 324, 119
- Yuan, F., Wu, M., & Bu, D. 2012, *Astrophysical Journal*, 761, 129
- Yuan, F., & Narayan, R. 2014, *Ann. Rev. Astron. Astrophys.*, 52, 529
- Yuan, F., Gan, Z., Narayan, R., et al. 2015, *Astrophysical Journal*, 804, 101